Electronic Materials Letters, Vol. 2, No. 1 (2006), pp. 1-5

Luminescent Properties of $LaMgAl_{11}O_{19}:Eu^{2+}$ Phosphor with a Structure of Distorted Magnetoplumbite and Its Thermal Stability for PDP Applications

Won Bin Im, Yu-HoWon, Yong-Il Kim[1], Ho Seong Jang, and Duk Young Jeon*

Department of Materials Science and Engineering, Korea Advanced Institute of Science and Technology, Daejeon 305-701, Korea
[1]Korea Research Institute of Standards and Science, Daejeon 305-600, Korea

We have evaluated the thermal stability of $LaMgAl_{11}O_{19}:Eu^{2+}$ ($LAM:Eu^{2+}$) phosphor synthesized by a conventional solid-state reaction method for plasma display panel application. Variation in the concentration quenching process was observed depending upon the excitation source, i.e., 147 and 370 nm, and the critical transfer distance was calculated as 20.1 and 16.4 Å, respectively. When both $LAM:Eu^{2+}$ and $BaMgAl_{10}O_{19}:Eu^{2+}$ (BAM) were baked in air at 500 °C for 30 min, the relative decrease of photoluminescence (PL) intensity of $LAM:Eu^{2+}$ was much lower than that of BAM. Due to structure factor of $LAM:Eu^{2+}$ around Eu^{2+} ions, Eu^{2+} ions were protected from outer oxidizing atmosphere. Analysis of thermal stability revealed that the differences in thermal stability between $LAM:Eu^{2+}$ and BAM could be ascribed to crystal structure of $LAM:Eu^{2+}$, which shields for Eu^{2+} ions from the oxidizing atmosphere.

Keywords: phosphor, thermal stability, PDP, distorted magnetoplumbite

1. INTRODUCTION

The thermal stability of a plasma display panel (PDP) phosphor is an important property for the manufacture of PDP panels. For example, the most typical blue emitting phosphor $BaMgA_{l0}O_{17}:Eu^{2+}$ (BAM) suffers from degradation of luminance during burning of the binder contained in the phosphor paste at 500 °C for 30 min after it is applied on the back plate of the PDP. It is known that the degradation of BAM can be attributed to two main factors, Eu^{2+} is oxidized to Eu^{3+} and water intercalation occurs in the opened-layer of the BAM structure[1-5].

In our previous study, we studied the thermal stability of several blue emitting PDP phosphors and obtained experimental results indicating that there could be another channel for a phosphor to degrade during the burning of binder[6-8]. Specially, it is the possible that the crystal structure of a host lattice might have some influence on its thermal stability. In order to assess this hypothesis, we evaluated a distorted magnetoplumbite structure (DMP), $LaMgAl_{11}O_{19}:Eu^{2+}$ ($LAM:Eu^{2+}$), comparing the phosphor with commercial BAM phosphor.

Aluminates with a magnetoplumbite-type structure are strongly related to the sizes of the cations of β-alumina and the distorted magnetoplumbite structure[9,10]. In particular, $BaMgAl_{10}O_{17}$ (β-alumina) basically has a structure of sodium β-alumina ($NaAl_{11}O_{17}$) in which $(Na, Al)^{4+}$ are replaced with $(Ba, Mg)^{4+}$. Its structure consists of Al spinel blocks, $[(Al_{1-x}Mg_x)_{11}O_{16}]$, and conduction layers that affect the thermal stability of phosphor significantly during the baking process[11, 12]. Therefore, based on its structural information and our previous results, we expect that a phosphor with DMP structure will have good thermal stability during the manufacturing process of PDP. This is because the conduction layer of $LAM:Eu^{2+}$ is tightly sealed by Al ions as shown in Fig. 1. Furthermore, it has been reported that the excitation spectrum of BAM consists of two different parts, i.e. a host lattice absorption band for electron/hole pairs generation from 140 nm to 190 nm and direct absorption bands of Eu^{2+} ions from 240 nm to 310 nm[13]. Therefore, $LAM:Eu^{2+}$

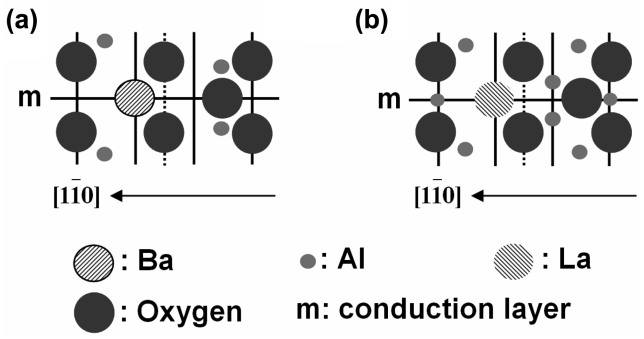

Fig. 1. Projection on the **[1$\bar{1}$0]** plane of conduction layer: (a) BAM and (b) DMP crystal structure.

*Corresponding author: dyj@kaist.ac.kr

having a spinel block in its crystal structure is also expected to have a good PL property under 147 nm excitation.

In this study, we synthesized LAM:Eu^{2+} phosphor of a single phase, and evaluated its thermal stability. Furthermore, using Rietveld refinement of LAM:Eu^{2+} against x-ray diffraction data, we attempted to determine whether there is any correlation between the crystal structure of the blue-emitting phosphor LAM:Eu^{2+} and its thermal stability during the baking process.

2. EXPERIMENTAL PROCEDURE

2.1 Sample preparation

Powder samples of LAM:Eu^{2+} were prepared by a conventional solid-state reaction. In order to synthesize LAM:Eu^{2+} phosphor, La_2O_3 (Kojundo, 99.99%), MgO (Aldrich, 99.99 %), Al_2O_3 (Sumitomo, 99.99%), and Eu_2O_3 (Aldrich, 99.99 %) were used as raw materials. Small quantities of BaF_2 were added as a flux. The raw materials were mixed using an agate mortar for 1 hour and subsequently heated at 1500 °C in a reducing atmosphere of H_2 (5%) and N_2 (95%) for 4 hours.

2.2. Photoluminescence (PL) measurement

The emission spectra of LAM:Eu^{2+} were obtained using a standard spectrometer setup DARSA PRO PL System (Professional Scientific Instrument Co, Korea), which utilizes a deuterium lamp as an excitation source. The sample chamber was maintained at about 5×10^{-5} torr using a turbo pumping system. PL spectra were obtained in a scanning wavelength region from 350 to 700 nm under excitation of 147 nm radiation from the deuterium lamp at room temperature. The excitation spectrum in the vacuum ultraviolet (VUV) region was corrected by sodium salicylate. In order to investigate the effect of the baking process on the luminescent property of LAM:Eu^{2+}, LAM:Eu^{2+} was baked at 500 °C in air for 30 min and compared with a commercial BAM treated in the same conditions.

2.3. Structural analysis of LAM:Eu^{2+} phosphor

The x-ray diffraction (XRD) data were obtained over the scattering angle in the range of $10^\circ \le 2\theta \le 130^\circ$ at a step of 0.02° using CuK_α radiation (Rigaku Dmax2200V). Rietveld refinement against the XRD data was made with the General Structure Analysis System (GSAS) program[14]. The experimental diffraction profiles were modeled by a pseudo-Voigt function within GSAS[15].

3. RESULTS AND DISCUSSION

3.1. Luminescent properties of LAM:Eu^{2+} phosphor

Figure 2 shows the PL excitation and emission spectra of LAM:Eu^{2+} phosphor under 147 nm excitation at room temperature, respectively. The emission spectrum is broad with a maximum at about 452 nm due to the transition of Eu^{2+} from the $4f^6 5d$ excited state to the $4f^7$ ground state. Because of the strong crystal field around Eu^{2+} ions, the lowest $5d$ level would become lower than the $^6P_{7/2}$ level. The emission peak of LAM:Eu^{2+} was observed at 452 nm[16]. The obtained CIE color coordinates of the synthesized LAM:Eu^{2+} were x = 0.1447 and y = 0.1105.

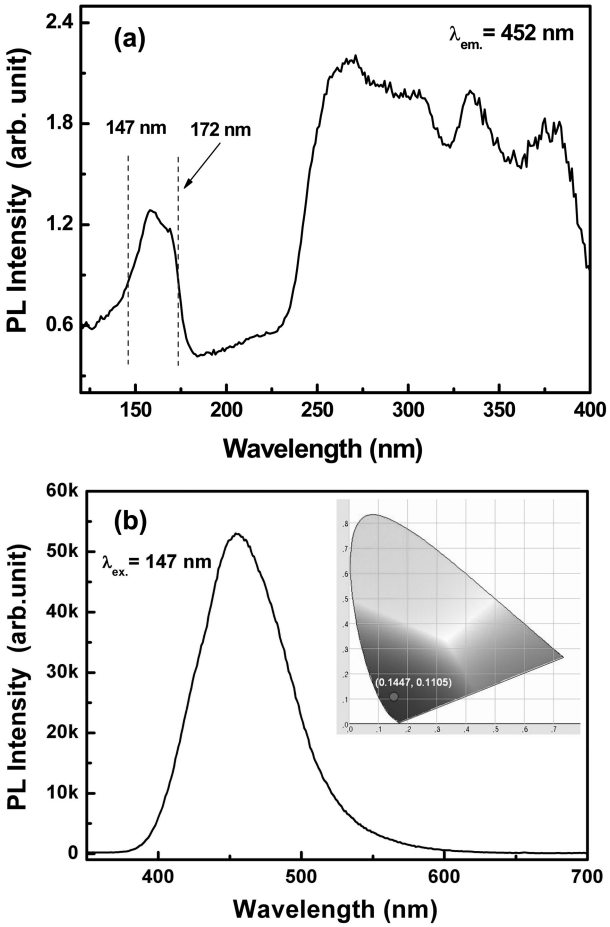

Fig. 2. (a) Excitation and (b) emission spectra of LAM:Eu^{2+} (λ_{ex} = 147 nm).

Figure 3 shows the relative PL intensity of LAM:Eu^{2+} phosphors as a function of concentration of Eu under excitation sources of 147 and 370 nm, respectively. As shown in Fig. 3, depending upon the excitation wavelength, the optimum concentration of Eu varied considerably. That is, the maximum PL intensity was obtained at 0.07 and 0.13 mol of Eu, corresponding to 147 and 370 nm, respectively. In order to understand the difference in the concentration quenching mechanism for different excitation sources, the critical distance (R_c) for energy transfer between the sensitizer and activator was calculated based upon the data of concentration quenching. In this case, the critical distance is equal to the average distance between the nearest activator ions corre-

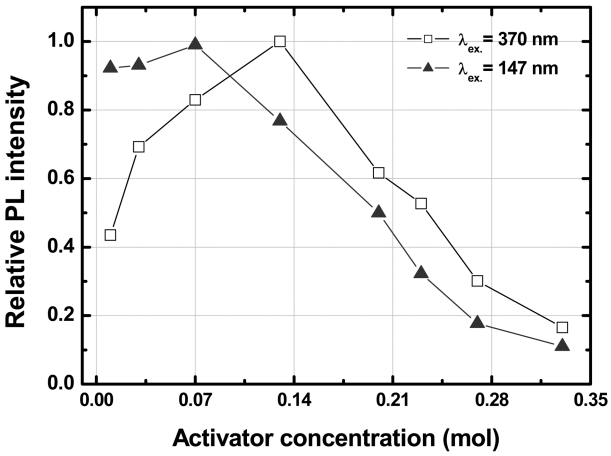

Fig. 3. Relative PL intensities of LAM:Eu^{2+} phosphor prepared with varying activator concentration (λ_{ex} = 147, 370 nm).

sponding to the critical concentration (X_c)[17]. The critical distance from the data of concentration quenching is represented as

$$R_C \approx 2\left(\frac{3V}{4\pi X_c N}\right)^{1/3} \quad (1)$$

Taking the values of V, N and X_c (V = 595.17 $Å^3$, N = 2, $X_{c,\ 147\,nm}$ = 0.07, $X_{c,\ 370\,nm}$ = 0.13, respectively), as given table in Table 1, the critical transfer distance of Eu^{2+} in LAM:Eu^{2+} was 20.1 and 16.4 Å, respectively. As calculated above, there are large differences between the VUV and direct excitation region in the energy transfer process. First, in the case of VUV excitation, the energy transfer process from the host lattice to the activator could play a significant role in the PL process. In VUV excitation, the excitation wavelength is shorter than the absorption edge of the host lattice, and thus the VUV spectrum does not excite an activator directly. Second, the VUV spectrum is very well absorbed into the host lattice such that its penetration depth into the phosphor particles is very small[18]. Depending upon the differences in the excitation source, variation in both the concentration quenching process and the energy transfer process was observed. For this reason, in the VUV region, a phosphor must have a property of high energy transfer from the host lattice to activators. If high phosphor efficiency under VUV excitation were obtained, the crystallinity of the host lattice would be a very critical factor.

In order to investigate the thermal stability of LAM:Eu^{2+}, LAM:Eu^{2+} and BAM were baked in air at 500 °C for 30 min, respectively. Figure 4 shows the relative PL intensities of LAM:Eu^{2+} and BAM before and after baking. In the case of

Table 1. Refined structural parameters for LAM:Eu^{2+} obtained from the Rietveld refinement using x-ray powder diffraction data at room temperature. The numbers in parentheses are the estimated standard deviations of the last significant figure

$LaMgAl_{11}O_{19}:Eu^{2+}$					
Atom	*x*	*y*	*Z*	*g*[a)]	U_{iso} /$Å^2$ [b)]
La	1/3	2/3	3/4	0.93[c)]	0.0091(2)[e)]
Eu	1/3	2/3	3/4	0.07[c)]	0.0091(2)[e)]
Al(1)	0.0	0.0	0.0	1.0	0.0094(7)
Al(2)	0.0	0.0	1/4	1.0	0.0395(6)
Al(3)	1/3	2/3	0.0283(4)	0.5[d)]	0.0025(1)[f)]
Al(4)	1/3	2/3	0.1891(1)	1.0	0.0073(1)
Al(5)	0.1674(2)	0.3349(5)	0.8914(5)	1.0	0.0081(2)
Mg	1/3	2/3	0.0283(4)	0.5[d)]	0.0025(1)[f)]
O(1)	0.0	0.0	0.1521(3)	1.0	0.0077(9)
O(2)	1/3	2/3	0.9407(1)	1.0	0.0066(8)
O(3)	0.1812(6)	0.3625(2)	1/4	1.0	0.0082(2)
O(4)	0.1514(8)	0.3029(6)	0.0533(1)	1.0	0.0029(5)
O(5)	0.5046(8)	0.0093(6)	0.1517(4)	1.0	0.0013(1)
Space group : $P6_3/mmc$ (No. 194) a = 5.5934(4) Å, b = 5.5934(4) Å and c = 21.9662(7) Å. α = 90 °, β = 90 °, and γ=120 °					

a) Occupation factor.
b) Isotropic atomic displacement factor.
c) Constraint on occupancy: g(La) + g(Eu) = 1.0.
d) Constraint on occupancy: g(Al) + g(Mg) = 1.0.
e) Constraint on isotropic atomic displacement factor: U_{iso}(La) = U_{iso}(Eu).
f) Constraint on isotropic atomic displacement factor: U_{iso}(Al) = U_{iso}(Mg).

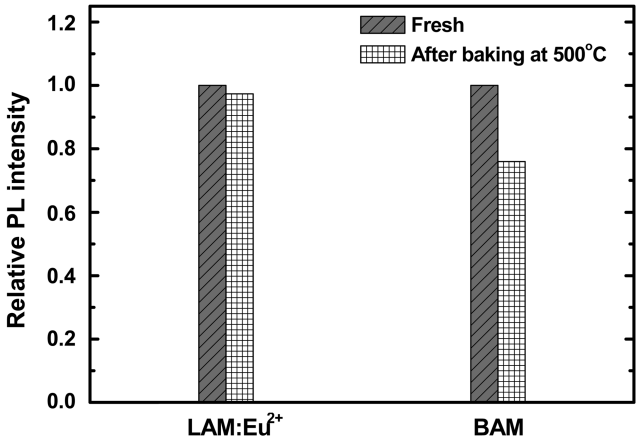

Fig. 4. Relative PL intensities of LAM:Eu^{2+} and BAM before and after the baking process at 500 °C for 30 min (λ_{ex} = 147 nm).

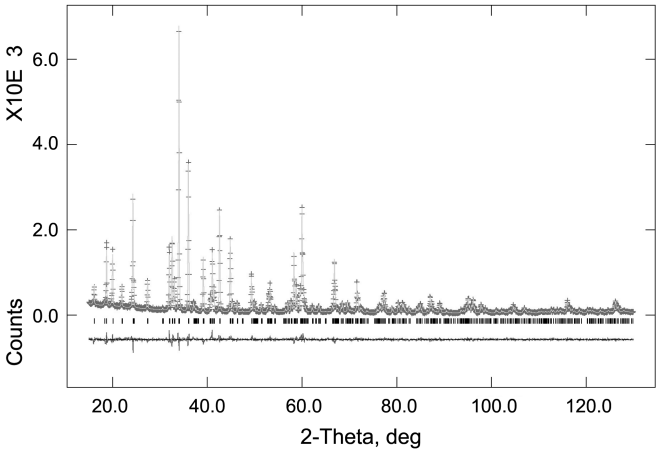

Fig. 5. Rietveld refinement patterns for LAM:Eu^{2+} x-ray powder diffraction data. Dots represent the observed intensities, and the solid line is calculated. A difference (obs. - cal.) plot is shown beneath. Tick marks above the difference data indicate the reflection positions.

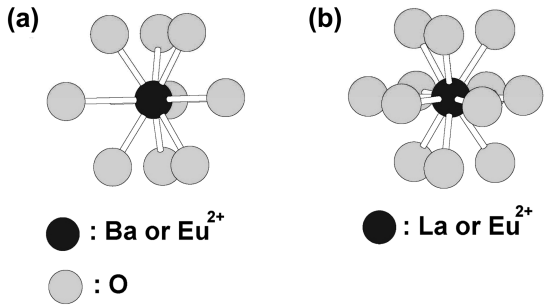

Fig. 6. Cation polyhedra arrangements of phosphor: (a) BAM and (b) LAM:Eu^{2+}.

BAM, the luminance was significantly reduced after baking at 500 °C, corresponding to a reduction of 25 %. However, in the case of LAM:Eu^{2+}, the PL intensity slightly decreased by about 2 %. Due to the structural shielding of closed-structure DMP in the conduction layer, it appears that Eu^{2+} ions are protected against the outer oxidizing atmosphere during the baking process.

3.2. Structural analysis of LAM:Eu^{2+} phosphor via Rietveld refinement

In our previous studies[19, 20], we reported that the average inter-atomic length of Eu^{2+}-oxygen ions ($d_{Eu\text{-}O}$) plays an important role in maintaining thermal stability during the baking process. Therefore, the Rietveld refinement against the XRD data was carried out so as to quantitatively investigate the sensitiveness of Eu^{2+} ions to the outer oxidizing atmosphere. A reasonable approximation of the actual crystal structure as a starting model is required in order to accomplish the crystal structural refinement. The starting structural model for LAM:Eu^{2+} was built with crystallographic data based on the *P6₃/mmc* space group[21]. The initial structural refinement cycles included the zero-point shift, the lattice parameters, the scale factor, and background parameters as variables. Following satisfactory matching of peak positions, the atomic positions, the thermal parameters, and the peak profile parameters including the peak asymmetry were refined. Si (NIST 640c) powder was used as an external standard to correct the zero-point shift for the measured diffraction data.

When Eu^{2+} ions are incorporated into the crystal structure of LAM, they may substitute all cationic sites, La^{3+}, Mg^{2+}, and Al^{3+}. However, considering their respective ionic radii and allowed oxygen-coordination number (n), i.e., Mg^{2+} (0.57 Å , n = 4), Al^{3+} (0.39 Å, n = 4), La^{3+} (1.03 Å, n = 8) and Eu^{2+} (1.25 Å, n = 8), Eu^{2+} ions can not readily substitute for Mg^{2+} or Al^{3+} ions[22]. Therefore, the structural refinement proceeded under the assumption that Eu^{2+} ions substituted only La^{3+} ions. The refined structural parameters for LAM:Eu^{2+} are listed in Table 1. The structural parameters for LAM:Eu^{2+} were successfully determined by the Rietveld refinement using XRD data. For LAM:Eu^{2+}, the final weighted R-factor, R_{wp}, was 9.08 % and the goodness-of-fit indicator, S (=R_{wp} / R_e), was 1.26. Figure 5 shows the Rietveld refinement results for LAM:Eu^{2+}.

As noted earlier with regard to the thermal degradation behavior of LAM:Eu^{2+} phosphor, its thermal stability is considerably superior to that of commercial BAM phosphor. The difference in thermal stability between LAM:Eu^{2+} and BAM can be ascribed to both crystal structures and the average inter-atomic length between Eu^{2+} and oxygen. Figure 6 shows the coordination polyhedra of Eu^{2+} (or La^{3+}) ions surrounded by O^{2-} ions for BAM and LAM:Eu^{2+}, respectively. As shown in Fig. 6, BAM and LAM:Eu^{2+} were constructed with coordination polyhedra consisting of Eu^{2+} ions surrounded by O^{2-} ions of 9- and 12-fold coordination, respectively. The average inter-atomic length between Eu^{2+} and

oxygen in BAM was 2.942(1) Å, while $d_{Eu\text{-}O}$ of LAM:Eu^{2+} was 2.734(1) Å. The difference in $d_{Eu\text{-}O}$ of the two crystal structures supports that the substitution of Eu^{2+} ions for the Ba^{2+} ions in BAM may be more sensitive to external environmental conditions such as temperature and oxidation atmosphere than in LAM:Eu^{2+}, because $d_{Eu\text{-}O}$ of BAM is longer than that of LAM:Eu^{2+}. Consequently, the thermal stability of the phosphors may be closely related to the crystal structures of the host materials, because the binding energy between Eu^{2+} and O^{2-} ions in relation with the mean inter-atomic distance depends upon their crystal structures.

4. CONCLUSIONS

We have synthesized blue-color emitting phosphor, LAM:Eu^{2+}, by a conventional solid-state reaction and evaluated its thermal stability. In addition, we also successfully determined its structure parameters by the Rietveld refinement method against x-ray powder diffraction data. Depending upon the difference in the concentration quenching process according to variation of the excitation source, the energy transfer mechanism of phosphor in the VUV region was considerably different from that in the UV region. Although the PL intensity of LAM:Eu^{2+} is lower than that of BAM, strong thermal stability was observed for LAM:Eu^{2+} during the baking process. From this study, it was confirmed that a host lattice having a non opened-structure and substitutional sites that allow for a short $d_{Eu\text{-}O}$ in a given host lattice should be considered as important conditions in terms of thermal stability during the baking process.

5. ACKNOWLEDGEMENTS

This study was supported by the Korea Science and Engineering Foundation (KOSEF) and the Ministry of Science & Technology (MOST) of the Korean government through its National Nuclear Technology Program.

REFERENCES

1. S. Oshio, T. Matsuoka, S. Tanaka, and H. Kobayashi, *J. Electrochem. Soc.* **145**, 3903 (1998).
2. T. H. Kwon, M. S. Kang, J. P. Kim, and G. J. Kim, *Proc. Int. Display Workshop'01,* p.1051 (2001).
3. B. Dawson, M. Ferguson, G. Marking, and A. L. Diaz, *Chem. Mater.* **16**, 5311 (2004).
4. P. Boolchand, K. C. Mishra, M. Raukus, A. Ellens, and P. C. Schmidt, *Phys. Rev. B* **66**, 134429 (2002).
5. K. S. Sohn, S. S. Kim, and H. D. Park, *Appl. Phys. Lett.* **81**, 1759 (2002).
6. W. B. Im, J. H. Kang, D. C. Lee, S. Lee, D. Y. Jeon, Y. C. Kang, and K. Y. Jung, *Solid State Commun.* **133**, 197 (2005).
7. W. B. Im, Y.-I. Kim, J. H. Kang, and D. Y. Jeon, *Solid State Comm.* **134**, 177 (2005).
8. W. B. Im, Y. -I. Kim, and D. Y. Jeon, *J. Mater. Res.* **20**, 2061 (2005).
9. A. L. N. Stevels and A. D. M. Schrama-de Pauw, *J. Electrochem. Soc.* **123**, 691 (1976).
10. S. R. Jansen, J. W. De Haan, L. J. M. Ven, R. Hanssen, H. T. Hintzen, and R. Metselaar, *Chem. Mater.* **9**, 1516 (1997).
11. Y.-I. Kim, S.-O. Kang, J.-S. Lee, M.-J. Jung, and K. H. Kim, *J. Mater. Sci. Lett*. **21**, 219 (2002).
12. A. L. N. Stevels, *J. Lumin.* **12/13**, 97 (1976).
13. G. Bizarri and B. Moine, *J. Lumin*. **113**, 199 (2005).
14. A. C. Larson and R. B. Von Dreele, *General Structure Analysis System (GSAS). Los Alamos National Laboratory Report LAUR.* **86**, 748 (1994).
15. L. W. Finger, D. E. Cox, and A. P. Jephcoat, *J. Appl. Cryst.* **27**, 892 (1994).
16. G. Blasse and B. C. Grabmaier, *Luminescent Materials.* p.49, Springer-Verlag (1994).
17. S. H. Shin, D. Y. Jeon, and K. S. Suh, *J. Applied Phys*. **90**, 12 (2001).
18. N. Youkosawa, G. Sato, and E. Nakazawa, *J. Electrochem. Soc.* **150**, H197 (2003).
19. W. B. Im, Y. -I. Kim, and D. Y. Jeon, *2005 International Meeting on Information Display,* p.1568 (2005).
20. W. B. Im, Y. -I. Kim, and D. Y. Jeon, *Chem. Mater.* (in press).
21. A. Kahn, A. M. Lejus, M. Madsac, J. Thery, D. Vivien, and J. C. Bernier, *J. Applied Phys.* **52**, 6864 (1981).
22. R. D. Shannon, *Acta Crystallogr. A* **32**, 751 (1976).